Backcalculation of asphalt pavement materials' moduli considering absolute and relative errors

Lia B. G. Furtado [1], Evandro Parente Jr.[1], Elias S. Barroso[1], Lucas F. A. L. Babadopulos[1], Samuel A. T. Silva[2], Juceline B. S. Bastos[3]

[1]*Departamento de Engenharia Estrutural e Construção Civil, Universidade Federal do Ceará*
Campus do Pici, Bloco 733, 60440-900, Fortaleza, Ceará, Brasil
liagomes@alu.ufc.br, evandro@ufc.br, elias.barroso@ufc.br, babadopulos@ufc.br
[2]*Laboratório de Mecânica dos Pavimentos, Universidade Federal do Ceará*
Campus do Pici, Bloco 734, 60440-900, Fortaleza, Ceará, Brasil
samuel@det.ufc.br
[3]*Instituto Federal de Educação, Ciência e Tecnologia do Ceará*
Av. Treze de Maio, 2081, 60040-531, Fortaleza, Ceará, Brasil
juceline.santos@ifce.edu.br

Abstract. Backcalculation is a procedure used to estimate the material properties of pavement layers from the results of non-destructive tests, such as the Falling Weight Deflectometer (FWD). Assuming that the behavior is linear elastic and the Poisson's ratios and layers thicknesses are known, the backcalculation procedure determines the elastic moduli that minimize the differences between the measured deflections and those computed using a finite element model. However, since the assumed geometry, material properties, and mechanical behavior are not identical to those of the actual pavement, the fitting is not perfect and the adopted error indicator (absolute or relative) affects the backcalculation process. The effect of the adopted error measure on the efficiency of the optimization method and backcalculated moduli is studied using numerical examples. The study uses the Finite Element Method with the CAP3D program to simulate pavement deflections under FWD testing. BackAP software is employed for backcalculating the elastic moduli of pavement layers, utilizing Gauss-Newton and Levenberg-Marquardt methods to solve a Nonlinear Least Squares problem. The research emphasizes the impact of error indicators - absolute versus relative - on the optimization process and accuracy. Results reveal that relative errors lead to more reliable backcalculated moduli across various pavement types. This highlights the importance of selecting appropriate error measures for accurate pavement analysis and material property assessment.

Keywords: Backcalculation, Asphalt Pavements, Fitting Error, Nonlinear Least Squares.

1 Introduction

Backcalculation estimates material properties from non-destructive tests, such as the Benkelman beam and the Falling Weight Deflectometer (FWD). It assesses pavement construction quality and monitors structural conditions. In an FWD test, an impulse load is applied to the pavement surface via a loading plate, and sensors (geophones) measure surface deflections at various offset. The measurement made by each geophone represents the deflection of the pavement structure at a particular location. Peak deflection is measured by the geophone directly below the load application point and deflections are smaller for more distant geophones [1].

The Finite Element Method (FEM) can be used to evaluate pavement deflections, based on known geometry, loading, and mechanical properties. Assuming linear elastic behavior and known Poisson's ratios, the backcalculation procedure consists of the determination of the elastic moduli that minimize the differences between the simulated and measured deflections.

The model fitting can be obtained by the minimization of the Sum of Squares of Errors (SSE), which consists of the Nonlinear Least Squares (NLS) problem. Several methods can be used to solve this problem [2, 3].

It is important to note that the geometry, material properties, and mechanical behavior assumed by the finite element model are not identical to those of the actual pavement. Furthermore, the measured deflections present inevitable errors due to the limited accuracy of actual sensors.

Thus, the fitting is not perfect and the adopted error indicator (absolute or relative), affects the the back-

calculation process since it corresponds to the objective function to be minimized by the optimization algorithm. Therefore, this work aims to study the effect of the adopted error measure on the efficiency of the optimization method and backcalculated moduli using numerical examples.

2 Finite Element Model

The FWD load (F) is applied at a circular loading plate of radius (r). Considering that the resulting pressure applied to the pavement is uniform

$$p = \frac{F}{\pi r^2} \tag{1}$$

and that the deflected region is much smaller than the pavement dimensions, the displacements, and stresses present axial symmetry. Therefore, in this work, the simulated deflections are computed using an efficient axisymmetric FE model with a mesh composed of quadratic finite (Q8) and infinite (L6) elements [4].

Numerical analyses are carried out using the CAP3D program [5]. The use of infinite elements allows to reduce of the number of finite elements and improves the displacements accuracy [4]. The mesh generation algorithm ensures that there is a node at the position of each geophone.

In FEM, the nodal displacement vector ($\mathbf{u}$) is computed by solving the linear system of equilibrium equations:

$$\mathbf{K}\,\mathbf{u} = \mathbf{f} \tag{2}$$

where ($\mathbf{K}$) is the global stiffness matrix and ($\mathbf{f}$) is the external load vector. The global stiffness of the FE model is assembled by the classical direct stiffness approach summing up the element stiffness matrices ($\mathbf{K}_e$):

$$\mathbf{K}_e = \int_{V_e} \mathbf{B}^T\,\mathbf{C}\,\mathbf{B}\,dV, \qquad \mathbf{C} = E\,\mathbf{A}(\upsilon) \tag{3}$$

where V_e is the element volume, $\mathbf{B}$ is the strain-displacement matrix, $\mathbf{C}$ is the elastic constitutive matrix, E is the modulus of elasticity, and $\mathbf{A}$ is a matrix depending only on the Poisson's ratio (υ) [6].

The NLS algorithms discussed in the next section require the gradients of nodal displacements. These derivatives can be computed by differentiation of eq. (2) with respect to parameter x_j:

$$\mathbf{K}\,\frac{\partial \mathbf{u}}{\partial x_j} = \mathbf{h}_j \quad \Rightarrow \quad \mathbf{h}_j = \frac{\partial \mathbf{f}}{\partial x_j} - \frac{\partial \mathbf{K}}{\partial x_j}\,\mathbf{u}. \tag{4}$$

It is important to note that $\partial\mathbf{f}/\partial x_j = \mathbf{0}$ since the external load vector does not depend on the material parameters. Furthermore, $\partial\mathbf{K}/\partial x_j$ can be exactly computed using finite differences, since $\mathbf{K}$ depends linearly on the modulus of elasticity (E), as shown in eq. (3). This procedure to exactly evaluate the displacement derivatives required by the NLS algorithms was implemented in the CAP3D program. It requires the solution of an additional linear system for each model parameter. Since the matrix K was already factored to solve eq. (2), the additional computational cost is small in comparison with a standard FE analysis.

3 Pavement Backcalculation

Pavement backcalculation can be written as a Nonlinear Least Squares (NLS) problem:

$$\min_{\mathbf{x}\,\in\,\mathbb{R}^n} f(\mathbf{x}) = \frac{1}{2}\sum_{i=1}^{m}\left(\frac{\hat{y}_i - y_i}{\overline{y}_i}\right)^2 = \frac{1}{2}\sum_{i=1}^{m} r_i^2 = \frac{1}{2}\mathbf{r}^T\mathbf{r}, \;\; n \le m \tag{5}$$

where $\hat{y}_i$ are the simulated deflections (FEM), y_i are the measured deflections (FWD), $\overline{y}_i$ are normalization factors, $\mathbf{r}$ is the residual vector, and

$$\mathbf{x} = \frac{1}{\overline{E}}\,[E_1, \cdots, E_n]^T \tag{6}$$

is the vector of unknown parameters, where E_j is the modulus of each pavement layer and $\overline{E}$ is a normalization factor. The Gauss-Newton and the Levenberg–Marquardt methods [2, 3] are applied in this work to solve the NLS problem.

3.1 Gauss-Newton

The Gauss-Newton (GN) method is obtained by the application of the Newton method to the NLS problem. The Newton method is based on a quadratic approximation of the function to be minimized:

$$f(\mathbf{x}_{k+1}) \approx f(\mathbf{x}_k) + \mathbf{d}_k^T \mathbf{g}_k + \frac{1}{2}\mathbf{d}_k^T \mathbf{H}_k \, \mathbf{d}_k, \tag{7}$$

where k is the iteration number, $\mathbf{d}$ is the search direction, $\mathbf{g} = \nabla f(\mathbf{x})$ is the gradient, and $\mathbf{H} = \nabla^2 f(\mathbf{x})$ is the Hessian matrix. The minimization of the approximate quadratic function yields:

$$\mathbf{g}_{k+1} \approx \mathbf{g}_k + \mathbf{H}_k \, \mathbf{d}_k = \mathbf{0}. \tag{8}$$

Thus, the search direction ($\mathbf{d}$) at each iteration k is evaluated solving the linear system:

$$\mathbf{H}_k \, \mathbf{d}_k = -\mathbf{g}_k. \tag{9}$$

If the Hessian is positive-definite then it can be easily shown that $\mathbf{d}_k$ is a descent direction ($\mathbf{d}_k^T \, \mathbf{g}_k < 0$) and the function value is reduced as we move in this direction.

The gradient and Hessian of the Sum of Squared Errors (SSE) function defined in eq. (5) are given by

$$\mathbf{g} = \mathbf{J}^T \mathbf{r}, \qquad \mathbf{H} = \mathbf{J}^T \mathbf{J} + \sum_{i=1}^{m} r_i \, \nabla^2 r_i, \tag{10}$$

where $\mathbf{J}$ is the Jacobian matrix:

$$\mathbf{J} = [J_{ij}] = \left[\frac{\partial r_i}{\partial x_j}\right] = \left[\frac{\partial \hat{y}_i}{\partial x_j}\right]. \tag{11}$$

The Gauss-Newton method is obtained neglecting the second term of the Hessian defined in eq. (10):

$$\mathbf{H} \approx \mathbf{J}^T \mathbf{J}. \tag{12}$$

After the computation of the search direction, the new estimate of the parameter vector is computed as

$$\mathbf{x}_{k+1} = \mathbf{x}_k + \alpha \, \mathbf{d}_k, \tag{13}$$

where α is the step size along the search direction. The classical Gauss-Newton method considers $\alpha = 1$.

In this work, a backtracking line search is adopted in order to improve the algorithm's robustness and efficiency. This algorithm starts with a unit step size ($\alpha_0 = 1$) and check the descent condition

$$f(\mathbf{x}_k + \alpha_l \, \mathbf{d}_k) < f(\mathbf{x}_k) + \alpha_l \, (\beta \, \mathbf{g}_k^T \mathbf{d}_k), \tag{14}$$

where l is the line search iteration and $\beta \in (0, 1)$ [2, 7]. If this condition is satisfied, the step size is accepted, otherwise, it is reduced:

$$\alpha_{l+1} = \eta \, \alpha_l \tag{15}$$

with $\eta \in (0, 1)$. The process is repeated until a sufficient function decrease is obtained. It is important to note that this approach allows for a unit step size at the solution, which is a condition for quadratic convergence of the Newton method. Furthermore, since the objective function is reduced at each iteration, the method will eventually converge to the local minimum.

The iterative process described in eq. (13) can be stopped when:

$$\text{NRMSE} = \sqrt{\frac{\mathbf{r}^T \mathbf{r}}{m}} < tol_1 \quad \text{or} \quad \|\mathbf{g}\| < tol_2, \tag{16}$$

where NRMSE is the Normalized Root Mean Square Error, while and tol_1 and tol_2 are the convergence tolerances.

The convergence rate of the Gauss-Newton method depends on how close eq. (12) approximates the true Hessian. Quadratic convergence can be obtained when the second term of the Hessian matrix, defined in eq. (10), is small close to the solution, which can occur when the residual is very small ($r_i \approx 0$) or the Jacobian is affine with respect to the parameters ($\nabla^2 r_i = 0$) [2].

3.2 Levenberg–Marquardt

The Levenberg–Marquardt (LM) method [2, 3] was proposed as a more robust alternative to the Gauss-Newton method. It is based on eq. (9), but use a modified Hessian:

$$\mathbf{H}_k = \mathbf{J}_k^T \mathbf{J}_k + \lambda_k \mathbf{I} \tag{17}$$

where the damping parameter ($\lambda_k > 0$) ensures that the $\mathbf{H}_k$ is positive definite, generating a descent search direction $\mathbf{d}_k$ at all iterations.

It is important to note that, for large damping factors, $\mathbf{d}_k \approx -\mathbf{g}_k/\lambda_k$, which is a short step in the steepest descent direction. This is a good option if the current iterate $\mathbf{x}_k$ is far from the solution. On the other hand, eq. (17) reduces to eq. (9) when λ_k is very small, generating the same search direction as the Gauss-Newton method, which is very good in the final iterations when $\mathbf{x}_k$ is close to the solution and Gauss-Newton can present quadratic convergence. Since the damping factor controls not only the search direction but also the step size, the Levenberg–Marquardt method is used without line searches. However, the new iterate is accepted only if it decreases the error:

$$\begin{cases} \mathbf{x}_{k+1} = \mathbf{x}_k + \mathbf{d}_k, & \text{if } f(\mathbf{x}_k + \mathbf{d}_k) < f(\mathbf{x}_k) \\ \mathbf{x}_{k+1} = \mathbf{x}_k, & \text{otherwise.} \end{cases} \tag{18}$$

Convergence is checked using eq. (16).

Several schemes have been proposed in the literature to update the damping factor [3, 8, 9]. The main idea is to begin with a relatively large factor λ. If the step computed by eq. (17) decreases the error, then λ is decreased. Otherwise, λ is increased. In this work, the damping factor is updated as:

$$\begin{cases} \lambda_{k+1} = \lambda_k/\gamma_1, & \text{if } f(\mathbf{x}_k + \mathbf{d}_k) < f(\mathbf{x}_k) \\ \lambda_{k+1} = \lambda_k\,\gamma_2, & \text{otherwise,} \end{cases} \tag{19}$$

where λ_0, γ_1, and γ_2 are positive real numbers.

3.3 Scaling and error indicator

The objective function (f) and the parameter vector ($\mathbf{x}$) used in the backcalculation process are normalized, as shown in eqs. (5) and (6). Normalization simplifies the definition of convergence tolerances, makes the problem independent of the adopted system of units, and improves the problem scaling.

It is important to note that better scaling improves the performance of gradient-based optimization algorithms [10]. Thus, in this work the normalization factor $\overline{E}$ is defined to bring the parameters x_j close to 1, avoiding working with large values. For instance, $\overline{E} = 10^9$ Pa is used for SI units.

On the other hand, the definition of deflection normalization factors $\overline{v}_i$ is more complex since they affect the error indicator to be minimized. To obtain consistent results and improve scaling, two different normalization schemes are used in this work depending on the chosen objective function. Thus, $\overline{y}_i = 10^{-3}$ is used as the normalization factor when the objective function is the absolute error, while the measured deflection is used as the normalization factor ($\overline{y}_i = y_i$) when the objective function is the relative error. Thus, the mean deflection is used as the normalization factor ($\overline{y}_i = \text{mean}(\mathbf{y})$) when the objective function is the absolute error, while the measured deflection is used as normalization factor ($\overline{y}_i = y_i$) when the objective function is the relative error.

4 Numerical Examples

The effects of the error indicator are assessed using numerical examples that consider relative and absolute errors. These examples are solved using BackCAP, a pavement backcalculation software based on the Finite Element Method and nonlinear optimization methods [11–13]. BackCAP is implemented in C++ using Object Oriented Programming (OOP) concepts. The program was modified to allow the use of the relative error as the objective function, as the original version considered only the absolute error.

The optimization parameters adopted in the numerical examples are:

- Stopping Criteria: $k_{max} = 100$, $tol_e = 10^{-6}$ (Sec. 4.1) and 10^{-3} (Sec. 4.2), $tol_g = 10^{-6}$.
- Gauss-Newton: $\beta = 0.2$, $l_{max} = 10$, $\eta = 0.5$.
- Levenberg-Marquardt: $\lambda_0 = 10^{-6}$, $\gamma_1 = 10$, $\gamma_2 = 10$.
- Bound Constraints: $\varepsilon = 10^{-2}$.

4.1 Pavement with different materials

This example consists of a pseudo-experimental problem corresponding to the backcalculation of the properties of three different pavement structures. The first is a well-designed structure with Hot Mix Asphalt (HMA) coating, simple graded gravel at the base, clayey soil at the subbase, on the silty subgrade. The second is a semi-rigid pavement, with graded gravel treated with cement used in the base, surpassing the stiffness of the upper layer, and the third is a defective structure, with poor compaction of the subbase, reducing its stiffness and making it less stiff than the subgrade.

Figure 1 summarizes these three pavements, showing the material properties, layer thicknesses, and the representation of the FWD test, including the applied load, the radius of the plate, and the position of each geophone. Table 1 presents the deflections for each pavement obtained by simulation using the finite element model. The seed moduli used are $E_0 = [3000; 280; 140; 190]$ MPa, based on the recommendations of the FHWA [14].

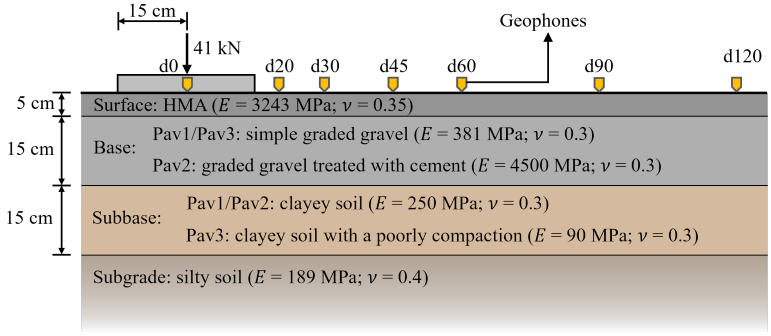

Figure 1. Schematic representation of the pseudo-experimental problem

Table 1. FWD deflections obtained by FEM

Model	Deflections (μm)						
	d0	d20	d30	d45	d60	d90	d120
Pav1	441.445	268.638	191.629	133.363	101.277	66.7199	49.0573
Pav2	223.192	182.327	159.393	129.566	105.198	71.2286	51.2071
Pav3	541.040	341.055	241.568	156.678	109.807	66.0115	47.7723

Both algorithms (GN and LM) were able to determine the exact moduli (shown in Figure 1) of the layers of each pavement for both absolute and relative minimization. This happens because the pseudo-experimental problem has a fitness error equal to zero at the end of the optimization process, then the normalization factor has no influence on the final result.

For Pav1, GN and LM required both 6 iterations for both normalization factors. For Pav2, GN and LM needed 9 iterations for absolute minimization and 10 for relative minimization. For Pav3, GN was more efficient, requiring 6 iterations for both normalization, while LM needed 12 for absolute and 13 for relative. The convergence behavior of the two algorithms is similar, but GN was more efficient for Pav3. The difference in the number of iterations was very small when comparing the absolute and relative minimization, showing that the adopted error indicator does not have a significant influence on the efficiency of this problem. Similar behavior is expected for backcalculation problems presenting small errors.

4.2 Four-layer highway pavement

This example consists of the backcalculation of an actual highway pavement where the FWD test was performed in 5 different locations. It is acknowledged that some authors in this subject have already indicated that backcalculation may have excessive uncertainty for pavements with asphalt layers thinner than 7.5 cm [14, 15]. The layer thicknesses, the representation of the FWD test, and the adopted Poisson's ratios are presented in Figure 2, while the applied load value, the recorded air and pavement surface temperatures, and the deflection basins are in Table 2. The seed moduli used are $E_0 = [2000; 100; 100; 100]$ MPa.

Table 3 presents the results obtained using both error indicators (absolute and relative), including the backcalculated moduli (no temperature correction was made for surface modulus (E_1), so the high temperatures recorded (Table 2) explain the low values in this modulus, considering the viscoelastic behavior of the material), the number

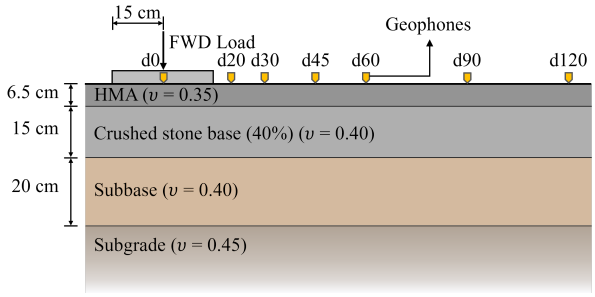

Figure 2. Schematic representation of the multi-layer highway pavement

Table 2. FWD data for a multi-layer highway pavement

st.	Temp. (oC)		F (kN)	Deflections (μm)						
	air	pav.		d0	d20	d30	d45	d60	d90	d120
1	34	45	46.383	290	159	107	68	47	29	23
2	33	47	45.851	843	517	342	209	143	73	44
3	34	49	45.851	843	517	342	209	143	73	44
4	34	47	45.693	1047	665	454	279	195	113	74
5	33	47	46.535	354	192	130	85	62	38	27

of iterations, the CPU time necessary to get these results for GN and LM algorithms and the NRMSE for both normalization procedures. These results show that the computational efficiency of both methods (GN and LM) is similar for the absolute error, but present a large variability for the relative error. Furthermore, the results indicate that the minimization of the relative error is much more difficult than the minimization of the absolute error. In this regard, GN was more robust as it successfully solved all stations for both errors, while LM was unable to solve the 4th station considering the relative error and the numerical parameters presented in Section 4.

Figure 3 shows the ratio between the moduli obtained minimizing the relative and absolute errors. As shown in this figure, the difference in subgrade modulus (E_4) is almost insignificant. On the other hand, very large differences (up to 40%) are observed for the upper layers, especially the surface and base courses. Therefore, the error indicator adopted in the backcalculation process does not only affects the convergence of the numerical algorithms but also the obtained solution.

Table 3. Backcalculated elastic moduli of the pavement sections' layers and corresponding processing parameters

st.	Min. Absolute									Min. Relative								
	Elastic Modulus (MPa)				Iter.		CPU time (s)		NRMSE	Elastic Modulus (MPa)				Iter.		CPU time (s)		NRMSE
	E_1	E_2	E_3	E_4	GN	LM	GN	LM	(%)	E_1	E_2	E_3	E_4	GN	LM	GN	LM	(%)
1	1691	708	300	447	6	6	2.2	2.0	0.06	2126	640	320	443	9	9	2.6	2.8	2.03
2	875	166	22	112	8	20	3.2	6.4	0.61	744	207	18	120	41	48	21.8	10.7	4.00
3	1276	254	56	171	8	9	3.3	3.0	0.59	995	355	41	188	44	56	24.8	13.2	5.16
4	1703	163	57	115	7	13	3.0	3.7	0.41	1022	224	46	120	11	-	3.7	-	2.98
5	1176	592	280	349	6	6	2.2	2.3	0.07	897	682	257	355	8	8	2.1	2.5	1.46

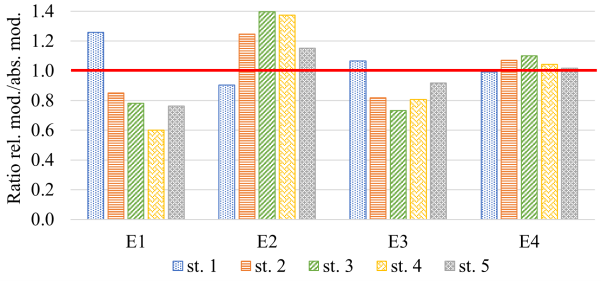

Figure 3. Ratio between the moduli obtained by relative and absolute minimization

5 Conclusion

This paper addressed the effects of the error indicator (absolute or relative) on the convergence of backcalculation algorithms and the obtained moduli of pavement layers. A very different behavior was obtained for pseudo-experimental and actual FWD tests.

The former problems present a perfect fit corresponding to zero absolute and relative errors. In this case, the expected solution was found by both Gauss-Newton and Levenberg-Marquadt methods, and the convergence behavior of these algorithms using absolute and relative error was similar.

On the other hand, backcalculation considering experimental FWD data does not present a perfect fit due to the difference in the actual loading, geometry, mechanical behavior, and material properties of the pavement layers and those considered in the finite element model. In this case, using a relative error leads to a harder-to-solve optimization problem. Furthermore, the differences in the backcalculated moduli obtained considering both error indicators may be significant, especially for the upper pavement layers.

Therefore, choosing absolute or relative error indicators has significant effects on the backcalculation process and obtained results. Due to its importance, this subject needs more in-depth studies.

Acknowledgements. The authors gratefully acknowledge the financial support provided by CNPq (Conselho Nacional de Desenvolvimento Científico e Tecnológico), CAPES (Coordenação de Aperfeiçoamento de Pessoal de Nível Superior) and FUNCAP (Fundação Cearense de Apoio ao Desenvolvimento Científico e Tecnológico).

Authorship statement. The authors hereby confirm that they are the sole liable persons responsible for the authorship of this work, and that all material that has been herein included as part of the present paper is either the property (and authorship) of the authors, or has the permission of the owners to be included here.

References

[1] Y. H. Huang. *Pavement analysis and design*. Pearson Prentice Hall, 2004.
[2] J. Nocedal and S. J. Wright. *Numerical Optimization*. Springer Series in Operations Research and Financial Engineering. Springer, New York, NY, 1999.
[3] K. Madsen, H. Nielsen, and O. Tingleff. *Methods for Non-Linear Least Squares Problems (2nd ed.)*, 2004.
[4] S. A. T. Silva, P. J. F. Vidal, Á. S. Holanda, and E. Parente Junior. Análise viscoelástica de pavimentos asfálticos utilizando elementos finitos e infinitos. *Transportes*, vol. 21, n. 3, pp. 5, 2013.
[5] de A. S. Holanda, de L. T. B. Melo, F. Evangelista, J. B. Soares, E. Parente, and de T. D. P. Araújo. An object-oriented system for finite element analysis of pavements. *III European Conference on Computational Mechanics*, pp. 178–178, 2006.
[6] K. J. Bathe. *Finite element procedures*. Klaus Jurgen Bathe, 2 edition, 2014.
[7] J. Arora. *Introduction to Optimum Design*. Academic Press, 2 edition, 2014.
[8] M. K. Transtrum and J. P. Sethna. Improvements to the levenberg-marquardt algorithm for nonlinear least-squares minimization, 2012.
[9] H. P. Gavin. *The Levenberg-Marquardt algorithm for nonlinear least squares curve-fitting problems*, 2020.
[10] P. E. Gill, W. Murray, and M. H. Wright. *Practical Optimization*. Society for Industrial and Applied Mathematics, Philadelphia, PA, 2019.
[11] E. S. Barroso, J. L. F. Oliveira, E. Parente Jr., L. F. A. L. Babadopulos, and J. B. S. Bastos. Efficient backcalculation procedure for asphalt pavements using the finite element method. *XLIII CILAMCE*, vol. , 2022.
[12] L. B. G. Furtado, E. Parente Jr, E. S. Barroso, L. F. A. L. Babadopulos, and J. B. S. Bastos. Solution of bound constrained nonlinear least squares problems with application to backcalculation of asphalt pavements. *XLIV CILAMCE*, vol. , 2023.
[13] L. B. G. Furtado, J. L. F. Oliveira, S. Lamothe, Éric Lachance-Tremblay, L. F. A. L. Babadopulos, J. B. S. Bastos, and E. Parente Jr. Efficient methodology for processing and using lightweight deflectometer data for on-site quality control of cement-bitumen treated materials. *International Conference on Asphalt Pavement ISAP*, vol. 1, 2024.
[14] L. M. Pierce, J. E. Bruinsma, K. D. Smith, M. J. Wade, K. Chatti, and J. M. Vandenbossche. *Using Falling Weight Deflectometer Data with Mechanistic-Empirical Design and Analysis, Volume III: Guidelines for Deflection Testing, Analysis, and Interpretation*. Federal Highway Administration, 2017.
[15] S. A. T. Silva, L. F. A. L. Babadopulos, J. L. F. Oliveira, J. B. Santos, E. Parente Jr., and L. B. G. Furtado. Effect of uncertainties in the input structural parameters and of arbitrary decisions by analysis on the results of backcalculated pavement's resilient moduli. *International Conference on Asphalt Pavement ISAP*, vol. 1, 2024.